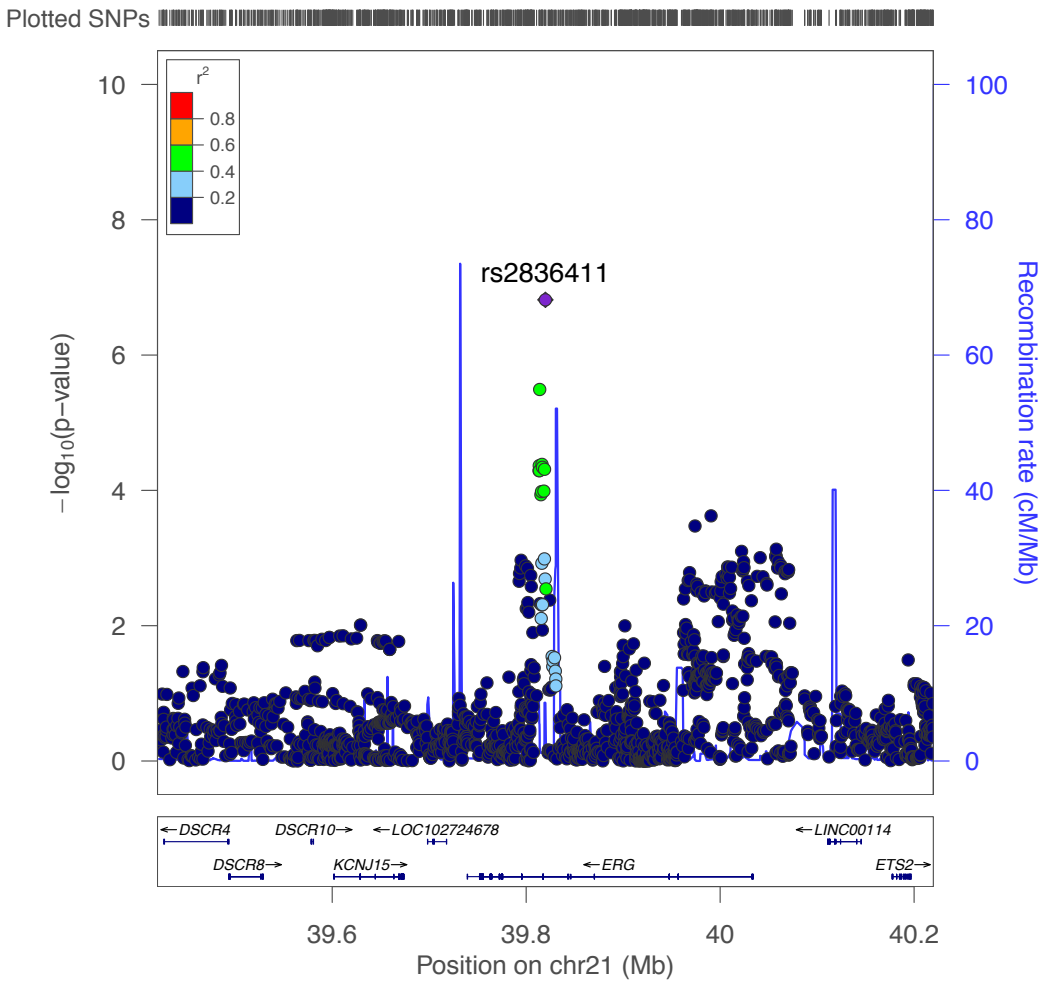

Supplementary Figure I. Regional association plot for rs2836411 for the abdominal aortic aneurysm (AAA) meta-GWAS. –log10 p-values from the AAA discovery meta-analysis of 6 GWAS datasets by Jones *et al*., 2017, are plotted against their genomic position using LocusZoom (1000Genomes, EUR, November 2014) (1). The colour indicates the linkage disequilibrium (r^2) with the peak SNP that is in purple. Gene names are indicated. Figure was obtained from Jones *et al*., 2017 (2).

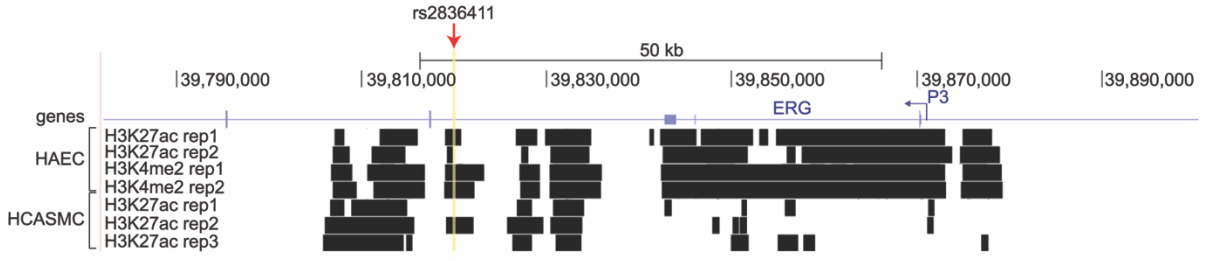

Supplementary Figure II. Comparison of H3K27ac and H3K4me1 peaks between vascular endothelial and smooth muscle cells. Peaks of H3K27ac and H3K4me2 for two replicates in human aortic endothelial cells (HAECs) from Hogan *et al*., 2017 (3) and of H3K27ac for three replicates in human aortic smooth muscle cells (HASMC) from Miller *et al*., 2016 (4) are shown together with UCSC genes and the location of rs2836411 (red arrow). The UCSC genome browser was used to generate this figure.

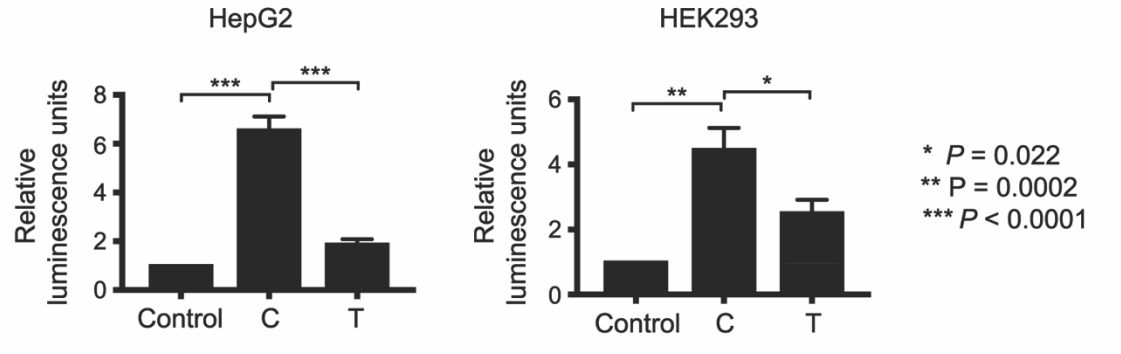

Supplementary Figure III. Luciferase enhancer assay in HepG2 and HEK293 cells show that the risk allele (T) of rs2836411 reduces enhancer activity. Allele-specific enhancer activity of rs2836411 compared to the control pGL4.23 vector was assessed using a luciferase reporter assay in HepG2 and HEK293 cells. The C variant (protective allele) harboured enhancer activity which was significantly reduced for the T variant (risk allele) in both cell lines. The average of 6 biological replicates +/- the standard error of the mean is shown. Statistical significance was determined by a one-way ANOVA followed by a Sidak's multiple comparisons test.

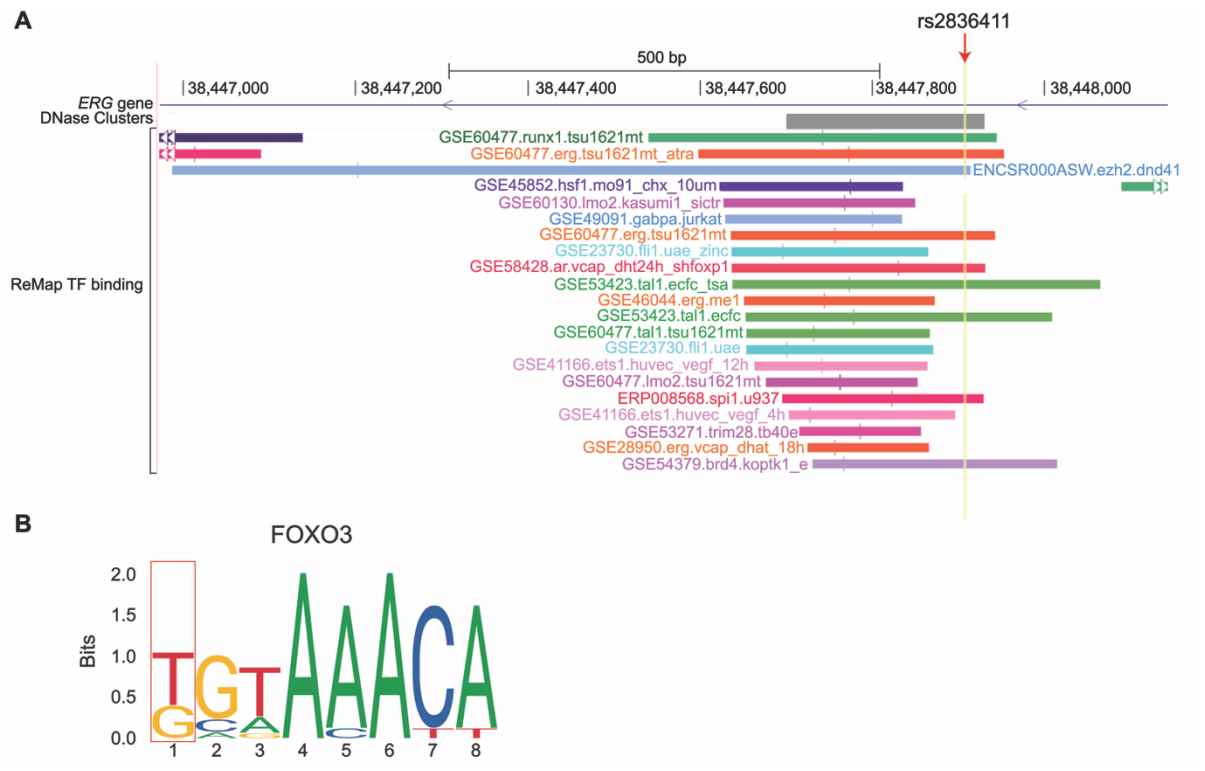

Supplementary Figure IV. Transcription factor binding and prediction of binding motif changes caused by rs2836411. (A) Transcription factor (TF) binding from published ChIP-seq studies is shown using the ReMap track (5) in the UCSC genome browser (assembly hg38), at the region surrounding rs2836411 (red arrow). DnaseI hypersensitivity clusters from ENCODE data is shown below the UCSC genes track. TF binding from ReMap lists for each binding site: 1) the GSE/ArrayExpress/ENCODE number of the data set, 2) the TF name, and 3) the biological condition (e.g. name of cell line). TSU-1621-MT is adult acute myeloid leukemia, DND-41 is T cell acute lymphoblastic leukemia, VCaP is human prostate cancer, ECFC: endothelial progenitor cell. KOPTK1: childhood T acute lymphoblastic leukaemia. ChIP-seq peak summits are represented by vertical bars. **(B)** rs2836411 is predicted to alter FOXO3 binding affinity. The binding affinity of FOXO3 is predicted to be altered by rs2836411 at position 1 (red square), with predicted binding scores by JASPAR of 7.93 vs. 10.8 for the C and T allele, respectively (6). The reference sequence to which FOXO3 is predicted to bind is CGAAAACA, with the position of rs2836411 underlined.

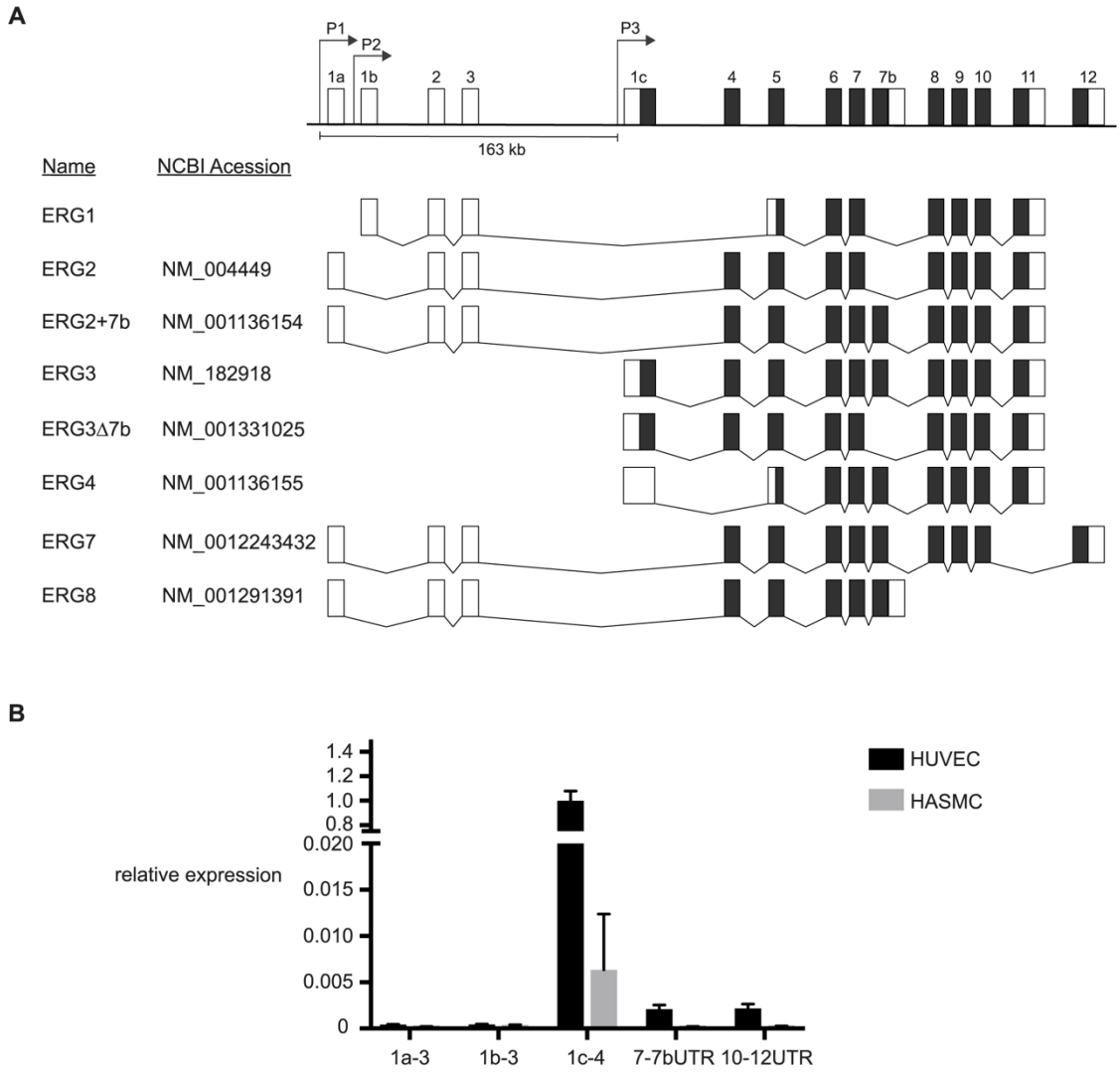

Supplementary Figure V. *ERG* isoform expression in HUVECs and HASMCs. (A) Schematic of the *ERG* gene structure and main isoforms found, with the P1, P2 and P3 promoters indicated by hooked arrows. Exons are indicated by boxes with 5' and 3' untranslated regions in white. Image was adjusted from Shah *et al*., 2016 (7) and Zammarchi *et al*., 2013 (8) and exons numbers and transcript names were obtained from these publications. **(B)** The expression of ERG isoforms in two different HUVEC lines and three different HASMC lines was measured by qPCR using exon-specific primers as listed on the x-axis. Expression values were normalised to the GeoMean of the reference genes *GAPDH* and *RPL13A* and are expressed relative to *ERG* exon 1c-4 in HUVECs. The mean +/- sem is shown.

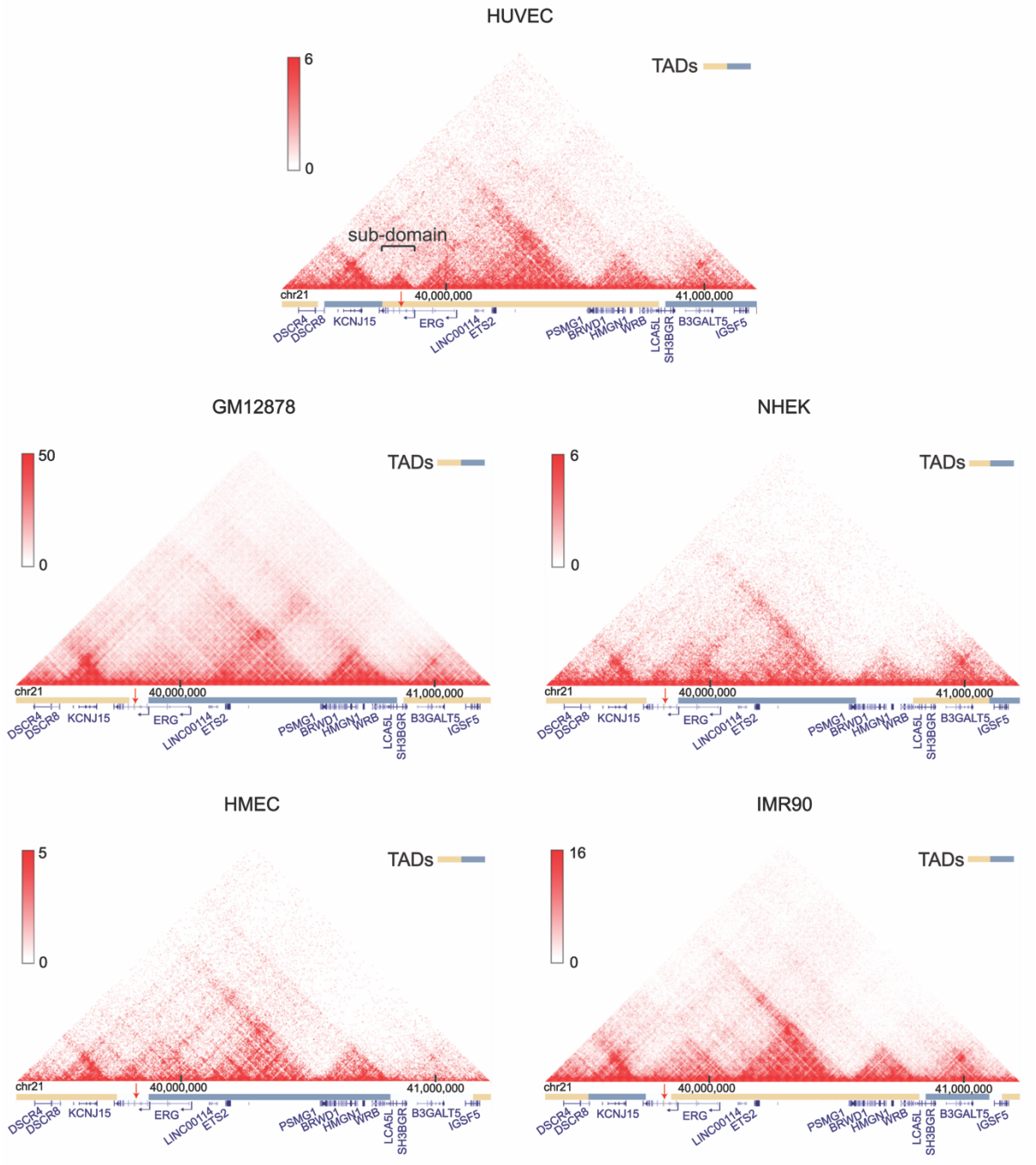

Supplementary Figure VI. Comparison of Hi-C data in HUVECs versus cell lines that do not express *ERG*. Hi-C contact maps with TADs indicated in HUVEC, GM12878, NHEK, HMEC and IMR90 cells from *Rao et al.*, 2014 (9) were obtained using the 3D genome browser (10). HUVECs express *ERG* and contain a sub-TAD (ST) from *ERG-P3* to the end of *ERG*, which is not pronounced at cell lines shown that do not express *ERG* (GM12878, NHEK, HMEC, IMR90). UCSC genes are shown below the TAD tracks, with the ERG P1/2 and P3 promoters indicated with hooked arrows and rs2836411 with a red arrow.

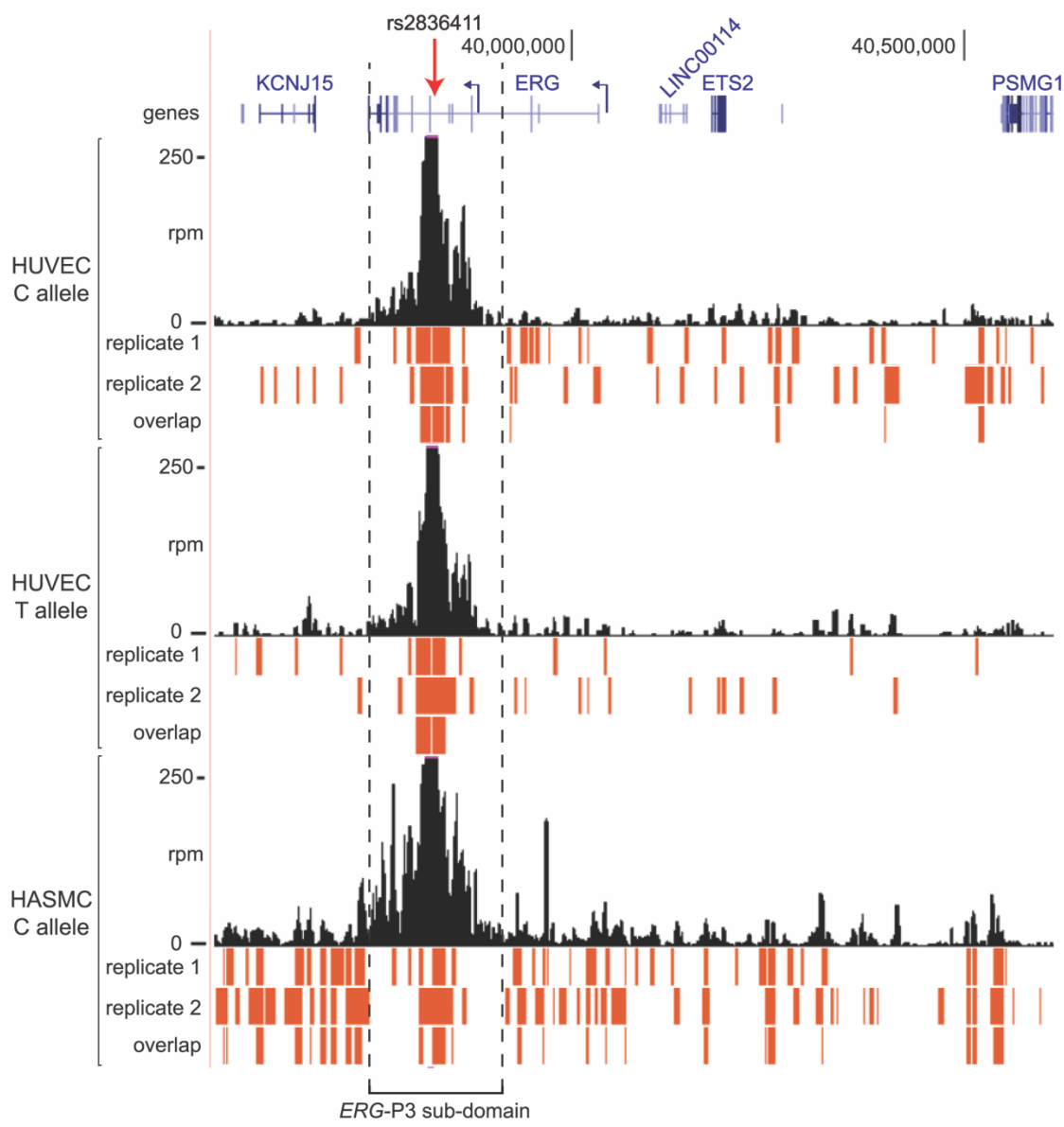

Supplementary Figure VII. 4C-seq significant interactions per replicate, and their overlap. 4C-seq profiles using a restriction fragment containing rs2836411 as a bait (red arrow) in HUVECs harbouring the C or T allele and in HASMCs homozygous for C allele. 4C-seq frequency tracks (black) represent the read per million (rpm) normalised running mean of 21 successive MseI restriction fragments for the average of two replicates and are shown together with statistically significant interactions (the top fifth percentile of interactions with a FDR of <0.01) per replicate, and the overlap between two replicates (red). Statistically significant interactions shown are of category 1 and 2 (see Material and Methods), and were called separately for the region within the *ERG-P3* sub-domain (region within the dotted lines) and on the total chromosome 21 (region outside the dotted lines). UCSC reference genes are in blue and the *ERG* P1/2 and P3 promoters are indicated by hooked arrows. Tracks were obtained using the UCSC genome browser.

Supplementary Table I. GTEx eQTL data for rs2836411 in vascular tissue types.

Gene Symbol	Gencode Id	P-Value	NES	T-statistic	Tissue
ERG	ENSG00000157554.14	0.0021	-0.15	-3.1	Artery - Aorta
ERG	ENSG00000157554.14	0.0079	-0.078	-2.7	Artery - Tibial
ERG	ENSG00000157554.14	0.013	-0.084	-2.5	Heart - Left Ventricle
LINC00114	ENSG00000223806.3	0.027	-0.14	-2.2	Artery - Tibial
ERG	ENSG00000157554.14	0.18	-0.049	-1.4	Heart - Atrial Appendage
KCNJ15	ENSG00000157551.13	0.18	0.052	1.4	Artery - Tibial
KCNJ15	ENSG00000157551.13	0.19	0.077	1.3	Heart - Atrial Appendage
PSMG1	ENSG00000183527.7	0.21	-0.058	-1.2	Artery - Aorta
ETS2	ENSG00000157557.7	0.27	-0.047	-1.1	Heart - Atrial Appendage
ETS2	ENSG00000157557.7	0.31	-0.044	-1	Heart - Left Ventricle
ETS2	ENSG00000157557.7	0.33	0.039	0.98	Artery - Aorta
KCNJ15	ENSG00000157551.13	0.42	-0.048	-0.81	Artery - Aorta
ETS2	ENSG00000157557.7	0.46	-0.022	-0.73	Artery - Tibial
PSMG1	ENSG00000183527.7	0.48	-0.032	-0.7	Artery - Tibial
KCNJ15	ENSG00000157551.13	0.49	0.052	0.68	Artery - Coronary
LINC00114	ENSG00000223806.3	0.66	0.035	0.44	Artery - Aorta
KCNJ15	ENSG00000157551.13	0.76	0.02	0.3	Heart - Left Ventricle
ETS2	ENSG00000157557.7	0.78	0.017	0.29	Artery - Coronary
PSMG1	ENSG00000183527.7	0.8	-0.012	-0.26	Heart - Atrial Appendage
PSMG1	ENSG00000183527.7	0.83	0.007	0.21	Heart - Left Ventricle
LINC00114	ENSG00000223806.3	0.88	0.015	0.15	Artery - Coronary
PSMG1	ENSG00000183527.7	0.97	0.0023	0.043	Artery - Coronary
ERG	ENSG00000157554.14	0.99	0.0011	0.016	Artery - Coronary
LINC00114	ENSG00000223806.3	NaN**	NaN**	NaN**	Heart - Atrial Appendage
LINC00114	ENSG00000223806.3	NaN**	NaN**	NaN**	Heart - Left Ventricle

* NES = normalised effect size.

** gene not sufficiently expressed for eQTL calculation.

Supplementary Table II. Primer sequences.

4C primers

Primer name	*Sequence (5´-3´)*
4C_MseI_6411_F	ACACTAGCCAGTGCCACCAT
4C_MseI_6411_R	CACCCATGATGAGAAACATGA

Primers used for cloning of rs2836411 DNA fragment

Primer name	*Sequence (5´-3´)*
Rs2836411-F	TGCAAAACAGATACTCCCTTCC
Rs2836411-R	TTTGCCAGATGTGAGAATGG

Primers used for quantitative PCR

Primer name	*Sequence (5´-3´)*
ERG-total-F	CCAGACACCGTTGGGATGAA
ERG-total-R	ATAGCGTAGGATCTGCTGGC
ERG-1a-3-F	CATGAGAGAAGAGGAGCGGC
ERG-1a-3-R	CTGACGGCTTTAGTTGCCCT
ERG-1b-3-F	GGCGCTAACCTCTCGGTTATT
ERG-1b-3-R	CTGTTCAGAACCTGACGGCT
ERG-1c-4-F	GCCAGCACTATTAAGGAAGCC
ERG-1c-4-R	TGTCCATAGTCGCTGGAGGA
ERG-7-7bUTR-F	ATGCTAGAAACACAGGGGGTG
ERG-7-7bUTR-R	GGTGTTTTCGTACCTGGCCT
ERG-10-12UTR-F	AAGTAGCCGCCTTGCAAAT
ERG-10-12UTR-R	GACCCAGTCCCAGAAGTCAC
GAPDH-F	TGCACCACCAACTGCTTAGC
GAPDH-R	GGCATGGACTGTGGTCATGAG
RPL13A-F	CCTGGAGGAGAAGAGGAAAGAGA
RPL13A-R	TTGAGGACCTCTGTGTATTTGTCAA

References

1 Pruim, R.J., Welch, R.P., Sanna, S., Teslovich, T.M., Chines, P.S., Gliedt, T.P., Boehnke, M., Abecasis, G.R. and Willer, C.J. (2010) LocusZoom: regional visualization of genome-wide association scan results. *Bioinformatics*, **26**, 2336-2337.

2 Jones, G.T., Tromp, G., Kuivaniemi, H., Gretarsdottir, S., Baas, A.F., Giusti, B., Strauss, E., Van't Hof, F.N., Webb, T.R., Erdman, R. *et al*. (2017) Meta-Analysis of Genome-Wide Association Studies for Abdominal Aortic Aneurysm Identifies Four New Disease-Specific Risk Loci. *Circ. Res.*, **120**, 341-353.

3 Hogan, N.T., Whalen, M.B., Stolze, L.K., Hadeli, N.K., Lam, M.T., Springstead, J.R., Glass, C.K. and Romanoski, C.E. (2017) Transcriptional networks specifying homeostatic and inflammatory programs of gene expression in human aortic endothelial cells. *Elife*, **6**.

4 Miller, C.L., Pjanic, M., Wang, T., Nguyen, T., Cohain, A., Lee, J.D., Perisic, L., Hedin, U., Kundu, R.K., Majmudar, D. *et al*. (2016) Integrative functional genomics identifies regulatory mechanisms at coronary artery disease loci. *Nat. commun.*, **7**, 12092.

5 Cheneby, J., Gheorghe, M., Artufel, M., Mathelier, A. and Ballester, B. (2018) ReMap 2018: an updated atlas of regulatory regions from an integrative analysis of DNA-binding ChIP-seq experiments. *Nucleic acids research*, **46**, D267-D275.

6 Khan, A., Fornes, O., Stigliani, A., Gheorghe, M., Castro-Mondragon, J.A., van der Lee, R., Bessy, A., Cheneby, J., Kulkarni, S.R., Tan, G. *et al*. (2018) JASPAR 2018: update of the open-access database of transcription factor binding profiles and its web framework. *Nucleic acids research*, **46**, D260-D266.

7 Shah, A.V., Birdsey, G.M. and Randi, A.M. (2016) Regulation of endothelial homeostasis, vascular development and angiogenesis by the transcription factor ERG. *Vascul. Pharmacol.*, **86**, 3-13.

8 Zammarchi, F., Boutsalis, G. and Cartegni, L. (2013) 5' UTR control of native ERG and of Tmprss2:ERG variants activity in prostate cancer. *PloS one*, **8**, e49721.

9 Rao, S.S., Huntley, M.H., Durand, N.C., Stamenova, E.K., Bochkov, I.D., Robinson, J.T., Sanborn, A.L., Machol, I., Omer, A.D., Lander, E.S. *et al*. (2014) A 3D map of the human genome at kilobase resolution reveals principles of chromatin looping. *Cell*, **159**, 1665-1680.

10 Wang, Y., Song, F., Zhang, B., Zhang, L., Xu, J., Kuang, D., Li, D., Choudhary, M.N.K., Li, Y., Hu, M. *et al*. (2018) The 3D Genome Browser: a web-based browser for visualizing 3D genome organization and long-range chromatin interactions. *Genome biology*, **19**, 151.